J. Pure Appl. & Ind. Phys. Vol.2 (3), 264-276 (2012)

Dielectric Studies on B-site Double Mixed Barium Titanate System

H. S. TEWARI and SAIKAT CHAKRABORTY*

Department of Pure and Applied Physics
Guru Ghasidas Vishwavidyalaya, Bilaspur – 495 009, INDIA.
*Department of Physics, Banaras Hindu University, Varanasi – 221005, INDIA.

(Received on : June 19, 2012)

ABSTRACT

Barium titanate having tetragonal structure with chemical formula ABO_3 is a ferroelectric perovskite oxide material at room temperature. For many years, A and B site doping have been used to modify the dielectric properties of BaTiO3 ceramics. The present work is undertaken with an objective to study the effect of partial substitution of Ti^{4+} by Mo^{6+} in barium titanate. In this work, two types of samples: $BaTi_{0.85}Mo_{0.10}O_3$ and $BaTi_{0.85}Mo_{0.15}O_{3+\delta}$ have been prepared using high temperature solid state ceramic method. In first composition of doping of Mo^{6+} is adjusted in such a way that there is no possibility of formation of vacancies in anionic or cationic sub lattices. In second composition, $BaTi_{0.85}Mo_{0.15}O_{3+\delta}$, the concentration of Mo^{6+} is chosen in such a fashion that charge compensation in perovskite structure occurs through formation of cationic vacancies or by excess oxygen in anionic sub lattices. X-ray diffraction patterns show the formation of single phase material. Both compositions show the normal ferroelectric transition in low temperature region and relaxor behaviour in high temperature range. The dielectric behaviour of these materials is explained on basis of creation of defects and presence of in-homogeneities at micro-level because of the low sintering temperature used for synthesis.

Keywords: Perovskites, Ferroelectrics, Dielectric properties, Defects.

1. INTRODUCTION

The extensive research in materials science and technology during the last couple of decades has led to great advances in understanding the properties of various unknown ceramics. Particularly mixed oxide ceramics have drawn attractions due to their

wide range of applications; cost effectiveness, easy process of fabrication and scope of improvement of materials properties with desired compositional modifications. One of the most extensively studied materials in this field is barium titanate, $BaTiO_3$. Tetragonal $BaTiO_3$ is a ferroelectric perovskite which exhibits high dielectric constant with Curie temperature (T_c) in the range of 120–130 ^oC. On heating, it undergoes a ferroelectric/paraelectric phase transition to the cubic structure at Curie temperature[6,16,17]. The phase transition is a first order and the peak in dielectric constant is correspondingly sharp[12]. $BaTiO_3$ is an important material due to its applications in multilayer ceramic capacitors (MLCC), positive temperature coefficient of resistance (PTCR), thermistors, piezoelectric sensors, transducers and electro-optic devices[2]. $BaTiO_3$ is a good substitute for lead containing compounds and environment friendly for various applications[13]. The relative simplicity of the perovskite structure led to a deeper understanding of the origin of ferroelectricity, quantitative phenomenological and first-principles modelling. Various attempts have been made to modify the properties of $BaTiO_3$ ceramics by substitutions at barium or titanium site or both sites. In fact, a large number of literatures are available on Barium site substitution in barium titanate, but a very limited report is available on heterovalent substitutions at Ti site[9,10,12,16]. The present work was undertaken with an objective of investigating the effect of partial substitution of titanium by a higher valence molybdenum ion and its effect on the dielectric characteristics of barium titanate. In present work, two types of compositions $BaTi_{0.85}Mo_{0.10}O_3$ and $BaTi_{0.85}Mo_{0.15}O_{3+\delta}$ have been synthesized. In first composition, concentration of doped Mo^{6+} is adjusted in such a way that there is no possibility of formation of vacancies in cationic or anionic sub-lattices. The cationic and anionic charges are compensated internally. The second composition, concentration of Mo^{6+} is chosen such that for charge compensation there is excess oxygen or cationic vacancies in perovskite lattice. The present report summarizes the results of an extensive study on the dielectric characteristics using complex plane impedance spectroscopy of $BaTi_{0.85}Mo_{0.10}O_3$ and $BaTi_{0.85}Mo_{0.15}O_{3+\delta}$ ferroelectric ceramics and their relative properties.

2. EXPERIMENTAL DETAILS

The $BaTi_{0.85}Mo_{0.10}O_3$ and $BaTi_{0.85}Mo_{0.15}O_{3+\delta}$ samples were prepared by conventional solid state mixed oxide route. Appropriate amounts of $BaCO_3$ (Merck 99%), TiO_2 (Loba Chemie 99.5%) and MoO_3 (John Barker 99%) were intimately mixed in acetone in an agate mortar and pestle for 05 hours. The mixed powders were placed in an alumina crucible at 700 °C for 03 hours and finally at 1000 °C in steps for 04 hours for calcinations in a high temperature furnace. The calcined powders were mixed with appropriate amount of poly vinyl alcohol and pressed in form of cylindrical pellets. These pellets were sintered in alumina boat at 1000 °C for 12 hours and furnace cooled to room temperature. The geometrical densities were measured for both compositions before and after sintering. X-ray diffraction (XRD) with Regaku table top model was used to

follow the progress of reaction and as indication of phase purity using Cu-K_α radiation (λ = 1.5405 Å) in the range $20°<2\theta<70°$ at room temperature. The sintered pellets were polished and coated with silver paste on both sides as electrode and cured at 100 °C for 03 hours. The dielectric parameters were measured as a function of frequency and temperature using HIOKI 3532-50 LCR Hi Tester for both compositions.

3. RESULTS AND DISCUSSION

Density and Lattice parameter determination

The density of both samples was measured before and after sintering using geometrical volume and weight of the pellets is given in Table. The X-ray diffraction patterns of both the samples show the formation of single phase material. The room temperature structure is tetragonal. The calculated values of the lattice parameters for both the compositions are given in Table-I.

Dielectric Properties

The variation of dielectric constant with temperatures at few selected frequencies for the compositions $BaTi_{0.85}Mo_{0.10}O_3$ (BTM) and $BaTi_{0.85}Mo_{0.15}O_{3+\delta}$ (BTM δ) are given in Fig. 1 (a) and 1 (b). For both samples at lower frequencies, dielectric constant first increases slowly with temperature then decreases to a particular temperature. Again after further increasing temperature, dielectric constant increases and attains a maximum value and thereafter decreases slowly. A broad peak appears for frequencies 0.5 kHz, 1 kHz, and 10 kHz. In case of $BaTi_{0.85}Mo_{0.10}O_{3,}$ dispersion in dielectric values is more pronounced in low temperature range. In both samples, the temperature at which dielectric peaks occurs at a measured frequency shift towards high temperature range with increase in frequency.

The variation of dielectric loss with temperature is shown in Fig 2(a) and 2(b) for both compositions. In case of $BaTi_{0.85}Mo_{0.15}O_{3+\delta}$ dielectric loss versus temperature plots show two peaks at a given frequency for all frequencies of measurement, one in low temperature region and another one in high temperature region. First peak occurs almost at same temperature at all frequencies of measurement but second peak shifts towards high temperature region with respect to first peak with increase in frequency.

Fig. 3(a) and 3(b) shows the variation of dielectric loss with frequency for both compositions. For composition $BaTi_{0.85}Mo_{0.15}O_{3+\delta}$, the plots show that dielectric loss (D) attain a peak (D_{max}) at all the measured temperatures, which shifts to a higher frequencies with increase in temperature and all curves merge at higher frequencies. The shifting of peaks towards higher frequency indicates that the relaxation time is decreasing with the increase in temperature. The peaks broadening with increasing temperature suggest the presence of temperature dependent electrical relaxation phenomenon in the material. The relaxation process is due to the presence of space charges whose mobility increases at higher temperature[10,15].

In case of $BaTi_{0.85}Mo_{0.10}O_3$, a peak is observed in dielectric loss versus log frequency plot, which shifts towards higher temperature region with increase in frequency. In this case the loss peaks occur in a narrow frequency range at all temperatures where as in case of $BaTi_{0.85}Mo_{0.15}O_{3+\delta}$, peak broadening increases with increase in temperature and decrease in peak value of dielectric loss is observed.

Impedance Studies

Figure 4(a) and (b) show the variation of log of real and imaginary parts of total impedance (Z' and Z'') as function of log of frequency, at various temperatures. The magnitude of Z' decreases with increase in frequency and temperature indicating an increase in ac conductivity with increase in temperature and frequency.

The Z' values at all temperatures seem to be merging at higher frequencies in Z' versus log f plot, due to release of space charge. In log Z'' versus log freq, Z'' peak starts appearing at all temperatures of measurements. These peaks are very broad and asymmetric at all temperatures. The peak shifts towards higher frequency with increase in temperature indicating the spread of relaxation times and the existence of temperature dependent electrical relaxation phenomenon. Asymmetric broadening of peak shows dominance of grain boundary relaxation processes at high temperatures[1,2,10].

Fig. 5(a) and 5(b) shows the variation of Z'' with frequency at different temperatures. A peak in Z'' values observed at higher temperatures of measurement. The peak broadening with increasing temperature for composition $BaTi_{0.85}Mo_{0.15}O_{3+\delta}$ indicates the presence of temperature dependent electrical relaxation phenomenon in the material and relaxation time is decreasing with the increase of temperature[3,7].

Fig. 6 shows the variation of relaxation time (log $\boldsymbol{\tau}$) with $10^3/T$ (K^{-1}). It appears to follow Arrhenius relation. The value of activation energy (E_a) as calculated from the slope of (log $\boldsymbol{\tau}$) versus $10^3/T$ curve is 0.19 eV for the composition $BaTi_{0.85}Mo_{0.10}O_3$ and 0.37 eV, 1.03 eV for the composition $BaTi_{0.85}Mo_{0.15}O_{3+\delta}$ in low and high temperature region respectively. The change in activation energy shows the change in conduction mechanism of the material. The value of activation energy for undoped $BaTiO_3$ is reported to be 1.56 eV[5,8,14,15]. Reduced activation energy implies high mobility of oxygen vacancies. In these materials, oxygen vacancies are considered as one of the mobile charge carriers. The ionization of oxygen vacancies creates conduction electrons which are easily thermally activated.

The distribution of relaxation frequency in the material may be attributed to cationic disorder due to the random distribution of B-site cations (Ti^{4+} and Mo^{6+}) having different ionic radii and valance state. The random distribution of B-site cations is responsible for wide distribution of relaxation times in $BaTi_{0.85}Mo_{0.15}O_{3+\delta}$ composition in comparison to composition $BaTi_{0.85}Mo_{0.10}O_3$ where random distribution of cations at B-site and creation of oxygen vacancies is restricted.

These materials are prepared by solid state ceramic method at high

temperature. we have used lower sintering temperature (~1000 ^{0}C) as comparison to required sintering temperature (~1250 ^{0}C), the phase formation and densification process may not be complete (below the limit of X-ray diffraction analysis) and affecting the dielectric behaviour of these materials.

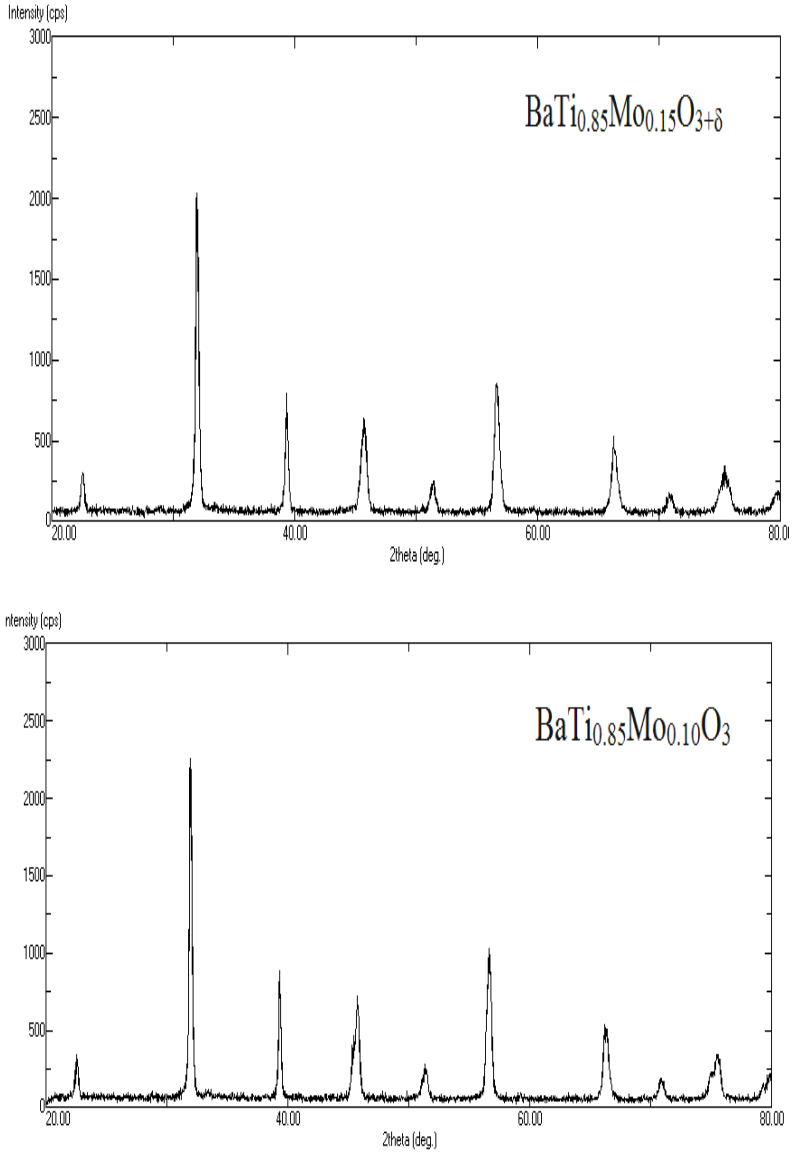

Fig. 1: XRD pattern of $BaTi_{0.85}Mo_{0.15}O_{3+\delta}$ (above) and $BaTi_{0.85}Mo_{0.10}O_3$ (below) samples.

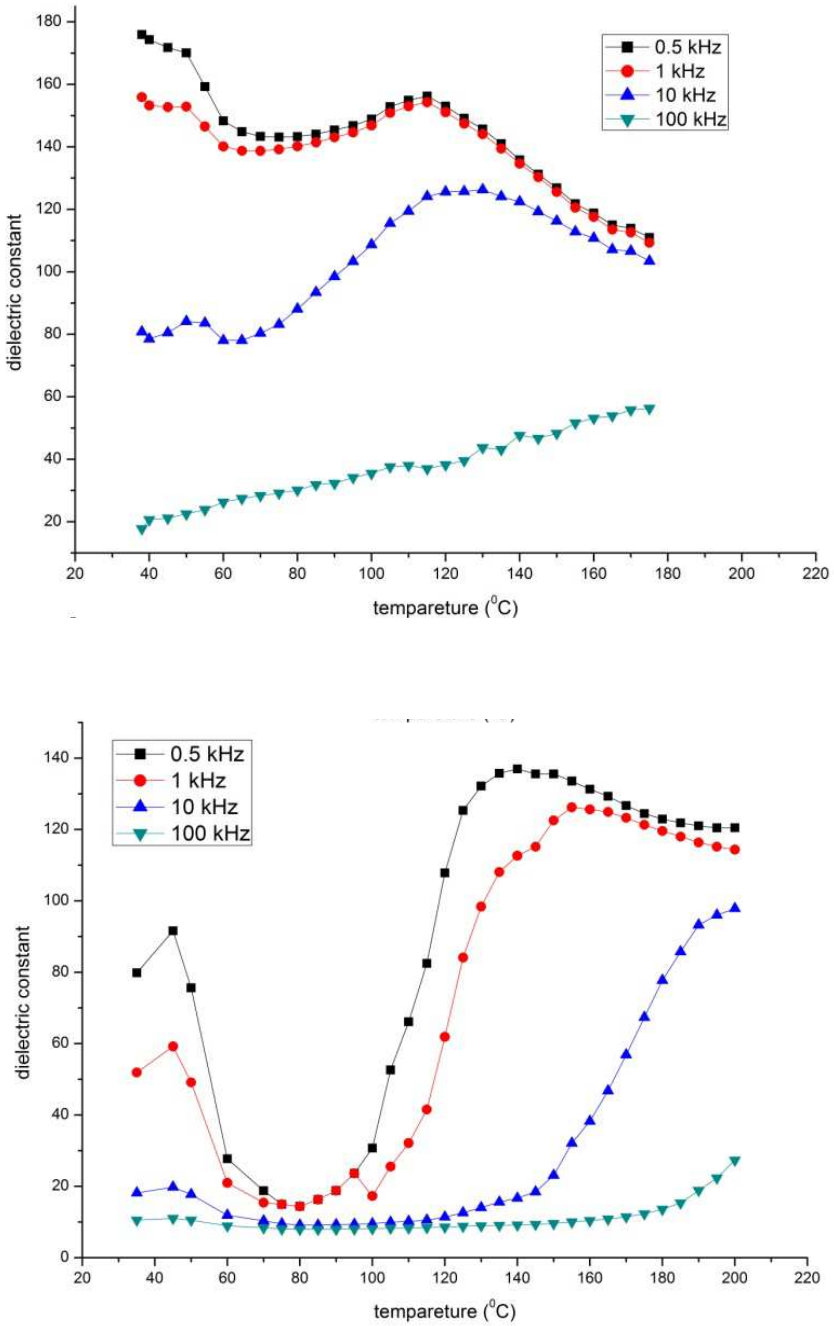

Figure 1: Temperature dependence of dielectric constant (ε) for (a) $BaTi_{0.85}Mo_{0.10}O_3$ (above) and (b) $BaTi_{0.85}Mo_{0.15}O_{3+\delta}$ (below).

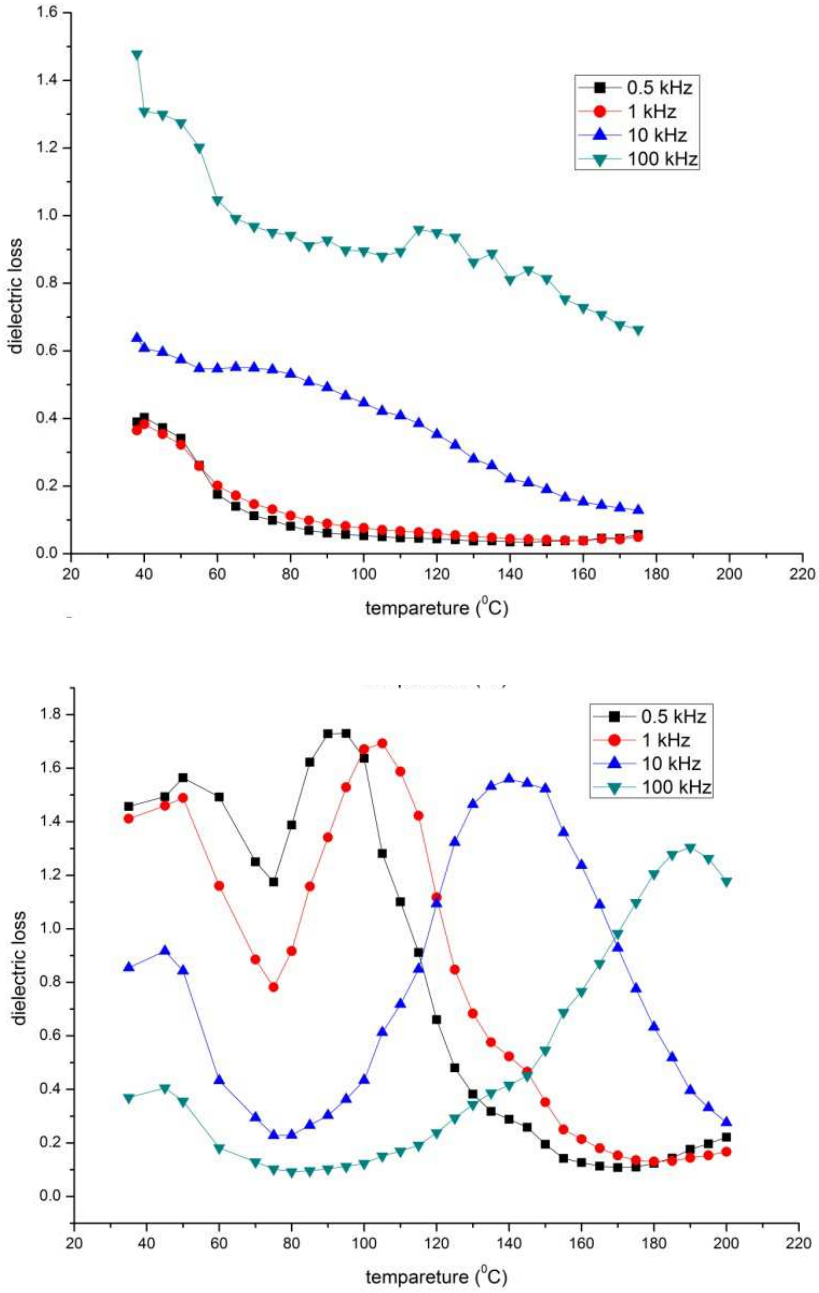

Figure 2: Temperature dependence of dielectric loss (tanδ) for (a) $BaTi_{0.85}Mo_{0.10}O_3$ (above) and (b) $BaTi_{0.85}Mo_{0.15}O_{3+\delta}$ (below).

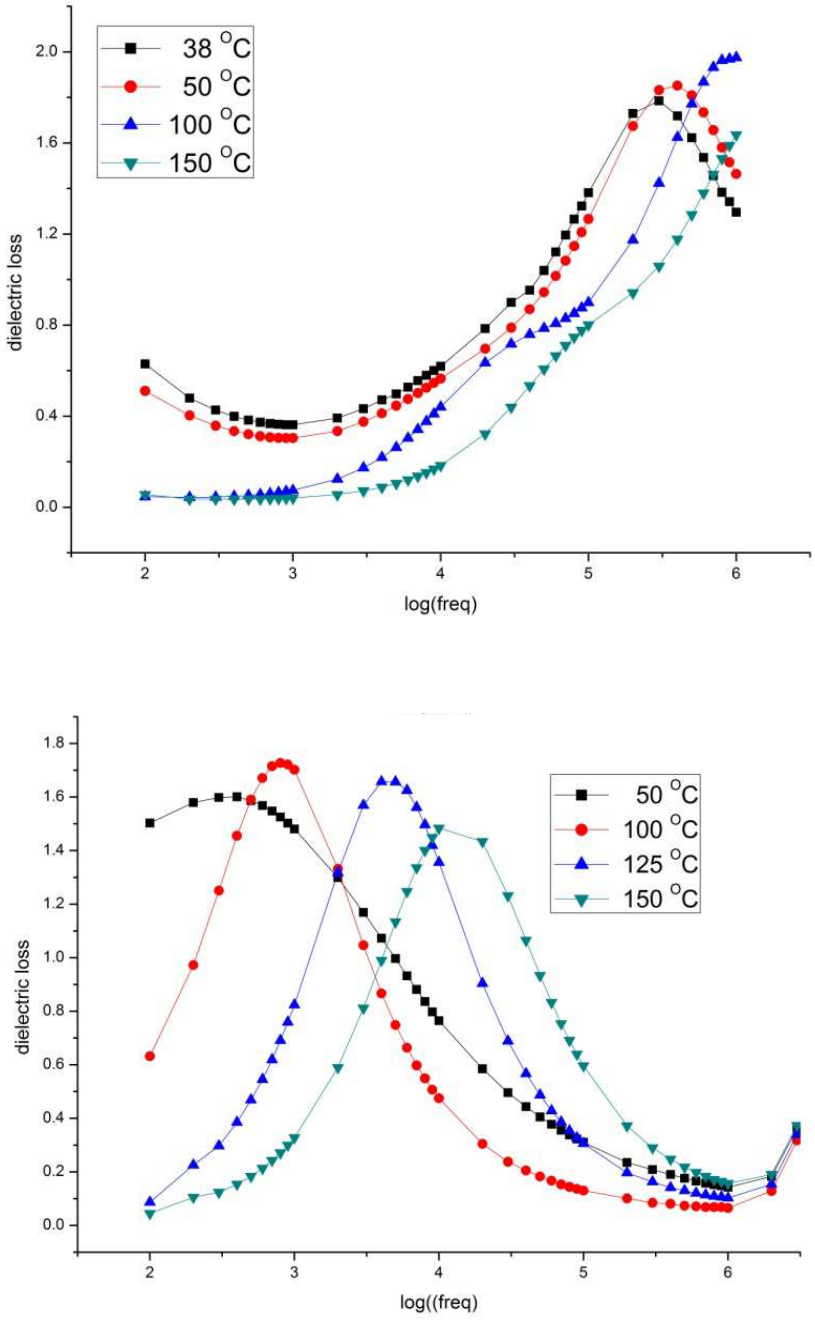

Figure 3: Frequency dependence of dielectric loss (tanδ) for (a) $BaTi_{0.85}Mo_{0.10}O_3$ (above) and (b) $BaTi_{0.85}Mo_{0.15}O_{3+\delta}$ (below).

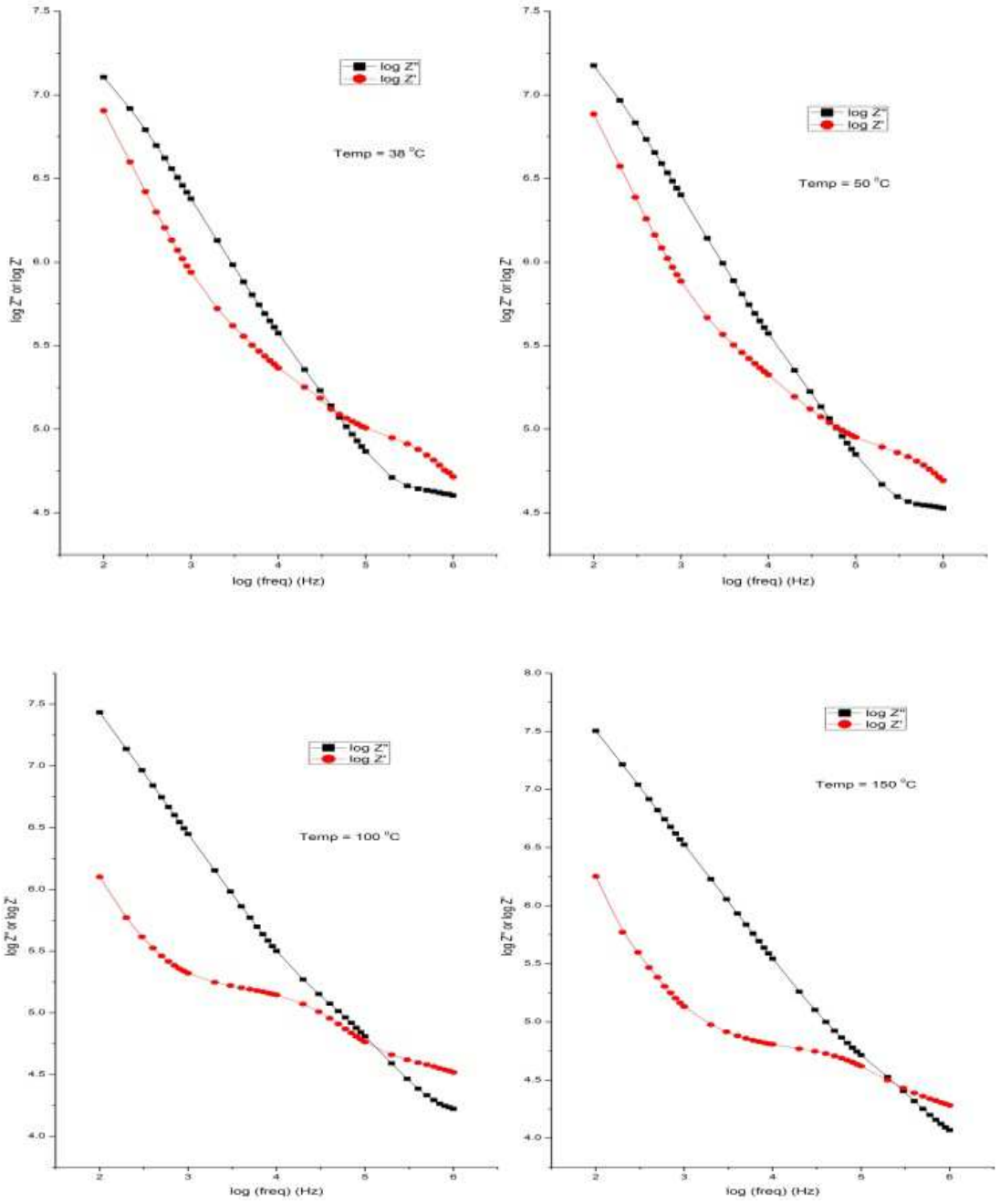

Figure 4(a): Variation of log of real and imaginary part of total impedance with log of frequency in $BaTi_{0.85}Mo_{010}O_3$.

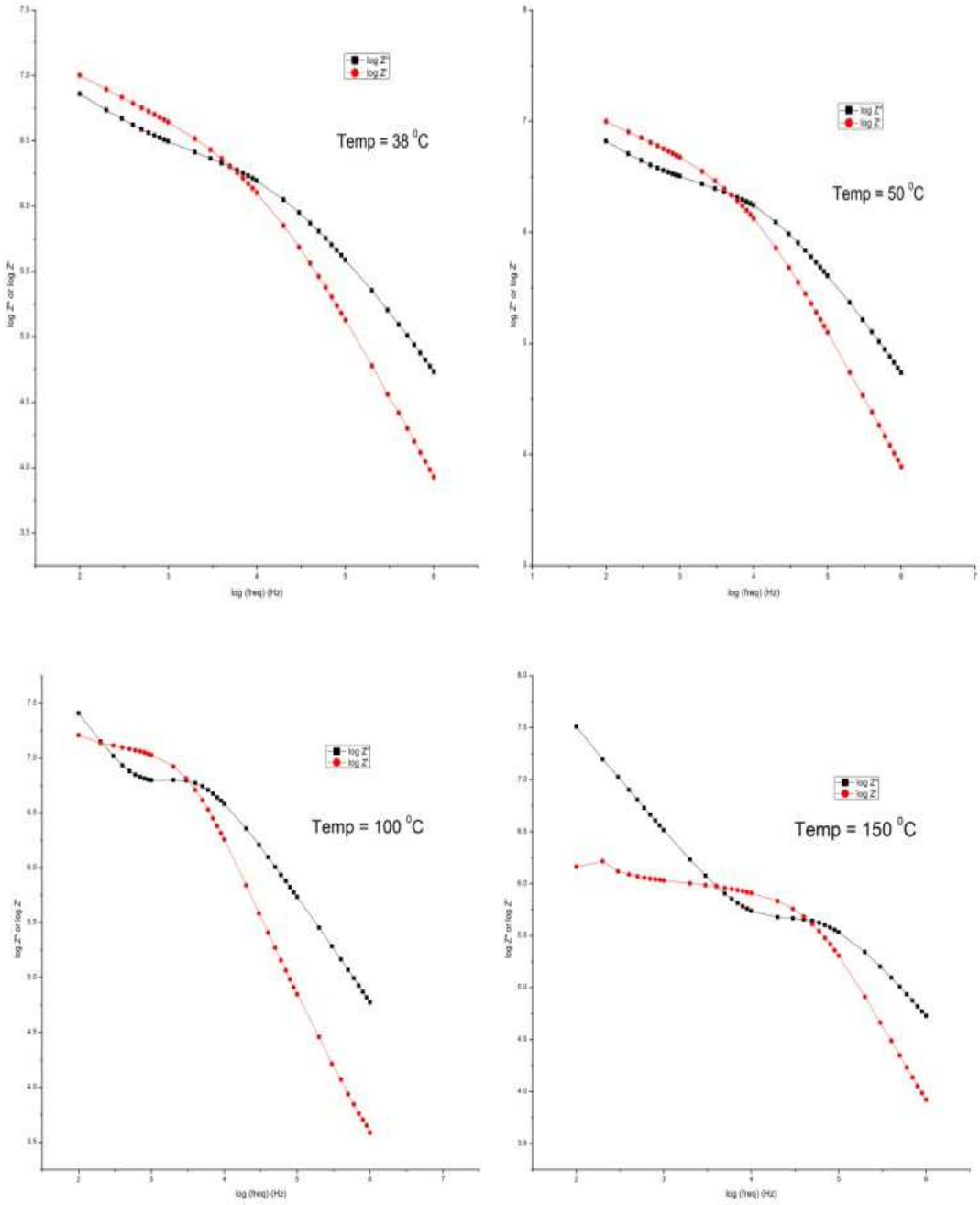

Figure 4(b): Variation of log of real and imaginary part of total impedance with log of frequency in $BaTi_{0.85}Mo_{0.15}O_{3+\delta}$.

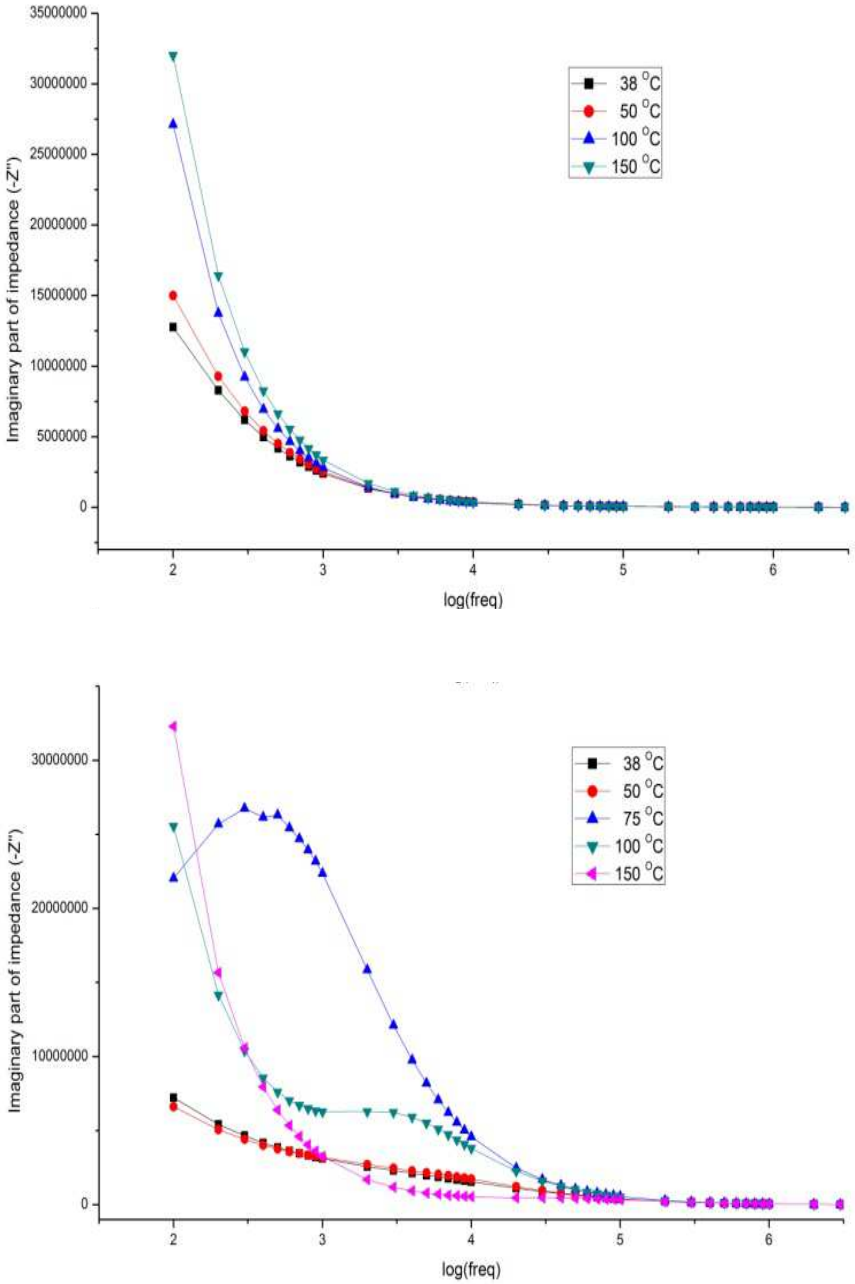

Figure 5: Frequency dependence of imaginary part of impedance (Z") for $BaTi_{0.85}Mo_{0.10}O_3$ (above) and $BaTi_{0.85}Mo_{0.15}O_{3+\delta}$ (below).

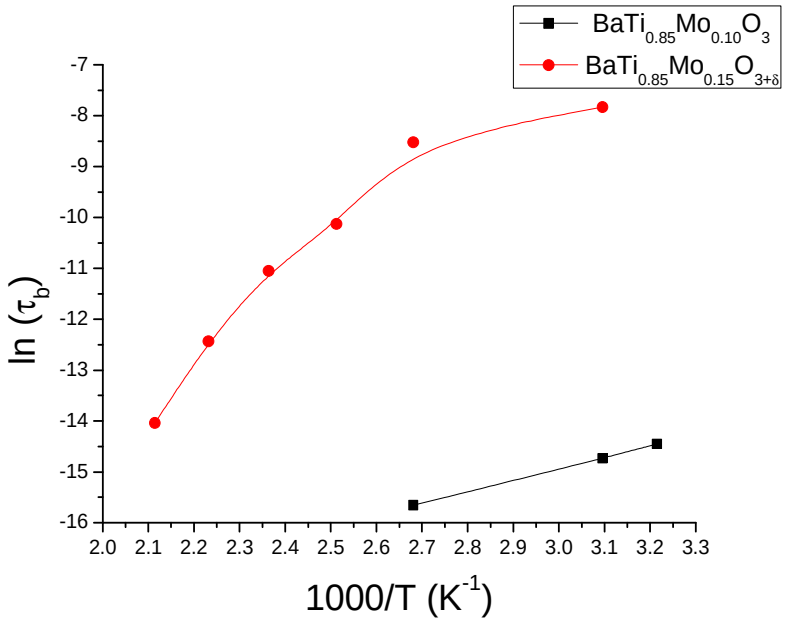

Figure 6: Variation of ln (τ_b) with inverse of absolute temperature (10^3/T) of $BaTi_{0.85}Mo_{0.10}O_3$ and $BaTi_{0.85}Mo_{0.15}O_{3+\delta}$.

Table-1: Density, Percentage Densification, Structure and Lattice Parameter of $BaTi_{0.85}Mo_{0.10}O_3$ (BTM) and $BaTi_{0.85}Mo_{0.15}O_{3+\delta}$ (BTM δ) compositions.

Samples composition	Time of measurement	Density [g/cc]	Densification	Structure and Lattice parameters
BTM	Before sintering	2.51	31%	Tetragonal a=b=3.928 Å c = 3.958 Å c/a = 1.008
	After sintering	3.66		
BTM δ	Before sintering	2.50	26%	Tetragonal a=b=3.935 Å c = 3.962 Å c/a = 1.007
	After sintering	3.38		

4. REFERENCES

1. A K Jonscher, R M Hill, C Pickup, *J. Mat. Sci*, 20, 4431 (1985).
2. Ashok Kumar, B. P. Singh, R.N.P. Choudhary and A. K. Thakur, *Materials Letters*, 59, 1880-1888, (2005).
3. B Behera, P Nayak and R N P Choudhury, *J. Alloys and Comp*, 436, 226-230, (2007).
4. B. P. Pokharel and D. Pandey, *J. of Appl. Phys*., 88, 5364-5373, (2000).
5. F. D. Morrison, D. C. Sinclair and A. R West, *J. Appl. Phys*., 86, 6355-59, (1999).
6. H. Jaffe, W. R. Cook and H. Jaffe, *Piezoelectric Ceramics*, Academic Press, London. (1971).
7. H. V. Alexandru, C. Berbecaru, A. Ioachin, L. Nedelcu, A. Dutta, *Appl. Surface Science*, 253, 354-357, (2006)
8. J. C. Burfoot, *Ferroelectrics*, (D. Vannostrond Company Ltd., London), (1967).
9. J. Ravez and A. Simon, *Eur. Phys. J., AP11*, 9, (2000).
10. Mahboob Syed, A.B. Duta, G. Swaminathan, G. Prasad and G. S. Kumar, *Ferroelectrics*, 326, 79-87. (2005)
11. Qiu S., Li W., Liu Y., Liu G., Wu Y. and Chen N., *Trans. Nonferrous Mat. Soc. China*, 20, 1911 – 1915, (2010).
12. R. Farhi, M El Marssi, A. Simon and J. Ravez, *Eur. Phys. J*., B9, 599-603, (1999).
13. R. T. Shrout *et al*., *J. Electroceram*., 19, 111-114, (2007).
14. S K Rout and J Bera, *Indian J. Phys*., 78, 819-822, (2004).
15. S. Devi and A. K. Jha, *Bull. Mater. Sci*., 33, 683-690, (2010),
16. S. Devi, P. Ganguly, S. Jain and A. K. Jha, *Ferroelectrics*, 381, 120-125, (2009).
17. W. J. Merz, *J. Appl. Physics*, 27, 938-35, (1956).